Chinese Journal of
POLYMER SCIENCE

RESEARCH ARTICLE

https://doi.org/10.1007/s10118-026-3662-1
Chinese J. Polym. Sci.

Influence of Salt on Swelling and Modulus of Polyelectrolyte Gels

Yi-Ming Liu[a], Jia-Dong Chen[a], Xian-Zhao Huang[b], Zhi-Xing Zhang[b], and Guang Chen[a,c*]

[a] *School of Advanced Manufacturing and Robotics, Peking University, Beijing 100871, China*
[b] *Industrialization Center of Micro & Nano ICs and Devices, Sino-German College of Intelligent Manufacturing, Shenzhen Technology University, Shenzhen 518118, China*
[c] *Key Laboratory of Polymer Chemistry and Physics of Ministry of Education, Peking University, Beijing 100871, China*

Abstract Polyelectrolyte (PE) gels are widely used in fields ranging from controlled drug delivery to tissue engineering, owing to their stimuli-responsive swelling behavior. The electrostatic interactions within the gels play a crucial role in the physical mechanisms underlying this response. In this work, we investigate the salt-dependent swelling behavior and shear modulus of PE gels based on a cell model, which explicitly addresses the inter-monomer electrostatic interactions. Through free energy minimization and asymptotic analysis, we derive four distinct scaling regimes for the equilibrium swelling ratio and modulus as functions of salt concentration, covering both overlapping and non-overlapping electric double layers. Comparisons between polyelectrolyte gels with different cross-link densities and charge intensities are also presented.

Keywords Polyelectrolyte gels; Stimuli-responsive swelling behavior; Shear modulus; Electrostatic interactions

Citation: Liu, Y. M.; Chen, J. D.; Huang, X. Z.; Zhang, Z. X.; Chen, G. Influence of salt on swelling and modulus of polyelectrolyte gels. *Chinese J. Polym. Sci.* https://doi.org/10.1007/s10118-026-3662-1

INTRODUCTION

Polyelectrolyte gels are polymer networks composed of cross-linked polyelectrolytes with ionizable groups.[1,2] Dissociation of ionizable groups leads to a charged polymer network, and the electrostatic interactions between the charged monomers and mobile ions result in the salt-dependent swelling behavior of PE gels.[3,4] This stimuli-responsive swelling property enables the widespread applications of PE gels, such as microrobots,[5,6] soft actuators,[7,8] and 4D printing.[9,10]

Numerous theoretical models have been proposed to describe the swelling behavior of PE gels. Flory and Rehner developed a theoretical framework to describe the swelling behavior of neutral polymer networks.[11,12] They determined the swelling equilibrium of the network by considering the balance between entropy of elastic deformation and polymer-solvent mixing. Subsequent studies extended the Flory-Rehner model to include electrostatic interactions in order to investigate the swelling behavior of polyelectrolyte gels. Katchalsky and co-workers modeled each PE chain as an isolated rod-like molecule, and presented the electrostatic free energy of a single chain by solving the linearized Poisson-Boltzmann (PB) equation.[13,14] While this model accounted for electrostatic effects on the swelling of PE gels in salt solutions, later studies pointed out that their analysis is restricted to the Debye-Hückel (DH) limit, which is valid only for small electrostatic potentials.[15,16]

Meanwhile, a Donnan potential has been broadly employed to capture the electrostatic potential difference between the gel and the external solution.[17–22] Nevertheless, the Donnan equilibrium assumes a uniformly distributed electrostatic environment inside the gel, thus neglects the polyelectrolyte effects associated with electrostatic interactions among charged polymer segments. Landsgesell *et al.* hierarchically coarse-grained the periodic gel model into a chain-based cell model, in which each cross-linked chain is represented as a ion-penetrable charged rod, and solved the electrostatic interactions within the PB framework.[16] Our recent work introduces a monomer-based cell model to depict the electrostatic interactions among charged monomers and mobile ions, and characterizes the salt-dependent swelling behavior of PE gels under conditions of overlapping electric double layers (EDLs).[23] The swelling behavior in this regime can also be captured by Donnan-based descriptions.

In this work, we extend our model to analyze the swelling of PE gels across both overlapping and non-overlapping EDLs, and further investigate the effect of salt concentration on the equilibrium modulus of the gel. Our approach resolves spatial variations of the electrostatic potential and ion distributions at the monomer level, thereby capturing inter-monomer electrostatic interactions.

THEORY

Free Energies

We consider a polyelectrolyte gel containing totally N monomers immersed in a solution reservoir with a salt concen-

* Corresponding author, E-mail: guangc@pku.edu.cn
Invited Research Article
Received February 5, 2026; Accepted March 11, 2026; Published online May 30, 2026

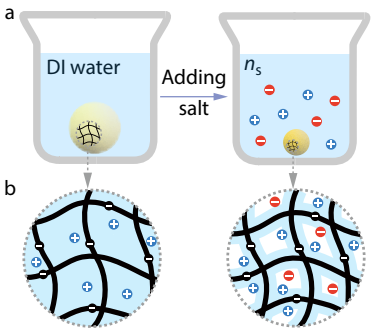

Fig. 1 (a) The schematic of salt-induced stimuli-responsive swelling behavior of PE gels; (b) Zoom-in illustration showing the electrostatic interactions among mobile ions and the charged polymer network; the blue region around each chain represents the electric double layers.

tration of n_s, as shown in Fig. 1(a). After free swelling, the gel reaches an equilibrium volume V, and shear modulus G. The swelling behavior of the PE gel is governed by the combined contributions of the network elasticity, excluded-volume effects, and electrostatic interactions.

The elastic free energy (F_{els}) of the gel is described using the neo-Hookean model, in which the polymer chains are treated as Gaussian, and the polymer-solvent mixture is assumed to be incompressible, thereby yielding

$$\frac{F_{els}}{k_BT} = \frac{3N}{2N_{str}}\left(\frac{V}{Nv}\right)^{\frac{2}{3}} \tag{1}$$

where k_B is the Boltzmann constant, T is the thermodynamic temperature, N_{str} denotes the number of monomers in a network strand (polymer segments between two adjacent cross-links), and v is the effective volume of a monomer.[24–26] In the presence of salt, the Gaussian-chain assumption is appropriate at the strand scale since the electrostatic repulsion is screened over the Debye length.[27] Therefore, network elasticity can be reasonably described based on Gaussian chain statistics in the present work. Although the finite extensibility effect may become non-negligible in highly swollen states, the neo-Hookean model captures the essential elastic response while remaining rather simple, and has therefore been widely adopted.[24,28,29]

According to Flory-Huggins theory,[25,30] for swollen gels with a small volume fraction $\phi = Nv/V \ll 1$, the excluded-volume energy F_{EV} takes the form

$$\frac{F_{EV}}{k_BT} = N\left[\left(\frac{1}{2}-\chi\right)\frac{Nv}{V} + \frac{1}{6}\left(\frac{Nv}{V}\right)^2\right] \tag{2}$$

where χ is the Flory-Huggins interaction parameter, which describes the interaction of the polymer chains with solvent molecules, as well as the binary interactions of polymer chains.

The electrostatic free energy (F_{elec}) is contributed by the electrostatic interactions between the charged polymer network and the surrounding mobile ions, as well as the entropy of mixing of the electrolyte ions. We employ a cell model, which models the charged monomers as similarly charged plates, cylinders, or spheres, to probe the electrostatic free energy of the PE gels. Such cell models have been extensively employed to investigate the properties of polyelectrolyte solutions and brushes.[31–34] Here, we assume that the monomers are homogeneously distributed in the gel, the volume of each cell is $\Omega = V/N$. We consider the case in which the monomers are negatively charged with a fixed charge fraction φ, so the charge density of each monomer is $\sigma = -e\varphi/A$, where e is the elementary charge, and A is the surface area of each monomer. The thickness of electric double layers formed near the monomer can be characterized by the Debye length $\lambda = \sqrt{\epsilon_0\epsilon_r k_BT/(2e^2n_s)}$, where ϵ_0 and ϵ_r are the vacuum permittivity and relative dielectric constant of water, respectively. In the framework of a mean-field description with point-like mobile ions, the electrostatic free energy F_{elec} takes the form

$$\begin{aligned}\frac{F_{elec}}{k_BT} = N\int_A \frac{\sigma\psi_s}{k_BT}\,dA - N\int_\Omega \frac{\epsilon_0\epsilon_r}{2k_BT}|\nabla\psi|^2 d\Omega + \\ N\int_\Omega \sum_i \left\{\frac{e\psi}{k_BT}z_i n_i + n_{i,\infty} + n_i\left[\ln\left(\frac{n_i}{n_{i,\infty}}\right) - 1\right]\right\} d\Omega\end{aligned} \tag{3}$$

where ψ denotes the electrostatic potential measured relative to the reservoir, *i.e.*, $\psi = 0$ in the bulk solution, ψ_s is the electrostatic potential at the monomer surface, $\nabla\psi$ denotes the gradient of the electrostatic potential, z_i represents the valence of ion species $i = \pm$, and n_i and $n_{i,\infty}$ denote local and bulk ion concentrations, respectively.

The Poisson-Boltzmann Equation

Since we consider the ions to be monovalent in the present work, we have $n_{\pm,\infty} = n_s$, $z_\pm = \pm 1$. Accordingly, taking functional variations of F_{elec} in Eq. (3) with respect to ψ and n_i leads to the Poisson equation and Boltzmann distribution

$$\frac{\delta F_{elec}}{\delta\psi} = 0 \Rightarrow \nabla^2\psi = -\frac{e(n_+ - n_-)}{\epsilon_0\epsilon_r} \tag{4a}$$

$$\frac{\delta F_{elec}}{\delta n_\pm} = 0 \Rightarrow n_\pm = n_s\exp\left(\mp\frac{e\psi}{k_BT}\right) \tag{4b}$$

The boundary condition at the charged surface (S) is determined by

$$\frac{\delta F_{elec}}{\delta\psi_s} = 0 \Rightarrow (\boldsymbol{n}\cdot\nabla\psi)_S = -\frac{\sigma}{\epsilon_0\epsilon_r} \tag{5}$$

Thus the electrostatic potential ψ can be evaluated analytically and numerically by solving Eqs. (4a)–(5).

Substituting ψ into the electrostatic free energy F_{elec} and minimizing the total free energy F with respect to the gel volume V, we obtain the swelling ratio $V/(Nv)$ of the PE gels at equilibrium state.

Shear Modulus

Our model can further be used to predict the equilibrium shear modulus of PE gels swelling in salt solutions with different concentrations. We use $G_0 = k_BT/(N_{str}v)$ to denote the shear modulus of the gel in the stress-free state.[24,25] For a neo-Hookean material, the Cauchy stress can be written as

$$\boldsymbol{\sigma} = \frac{G_0}{J}\left(\mathbf{F}\mathbf{F}^{\mathbf{T}} - \mathbf{I}\right) \tag{6}$$

where $\mathbf{F}$ is the deformation gradient, and $J = |\mathbf{F}|$.[35] To evaluate the modulus G of a swollen gel, we consider applying a small shear deformation on it. So the deformation gradient $\mathbf{F}$ is

$$\mathbf{F} = \alpha\begin{bmatrix}1 & \gamma & 0\\ 0 & 1 & 0\\ 0 & 0 & 1\end{bmatrix} \tag{7}$$

where $\alpha = [V/(Nv)]^{1/3}$ is the stretch ratio of the freely swollen

gel, γ is the shear strain. Substituting Eq. (7) into Eq. (6), we derive the shear stress

$$\tau = \sigma_{xy} = G_0 \alpha^{-1} \gamma \tag{8}$$

According to the definition of shear modulus $G = \tau/\gamma$, the modulus of a swollen gel can be written as

$$G = G_0 \left(\frac{V}{Nv}\right)^{-\frac{1}{3}} \tag{9}$$

This scaling is physically reasonable, as modulus is positively correlated with the cross-link density in the gel. The swelling of the gel dilutes the cross-link density, *i.e.*, the number of network strands per unit volume decreases, leading to a reduction of modulus.

Defining the dimensionless modulus as $Gv/(k_BT)$, Eq. (9) can be written as

$$\frac{Gv}{k_BT} = \frac{1}{N_{str}} \left(\frac{V}{Nv}\right)^{-\frac{1}{3}} \tag{10}$$

SCALING LAWS

We apply the planar cell model to describe the electrostatics within PE gels, and derive the analytical approximations of electrostatic free energy F_{elec}, swelling ratio $V/(Nv)$ and nondimensional modulus $Gv/(k_BT)$ through asymptotic analysis of the Debye length λ and electrostatic potential ψ.

Charged Polyelectrolyte Gels: $F \approx F_{els} + F_{elec}$

Over a broad range of salt concentrations, the excluded-volume free energy (F_{EV}) is negligible compared with the electrostatic free energy (F_{elec}), *i.e.*, the total free energy of the PE gel $F \approx F_{els} + F_{elec}$.

Considering the Debye length is much larger than the distance between monomers $\lambda \gg l$, *i.e.*, the EDLs are overlapped, we obtain an approximate solution for ψ and $n_\pm$ from Eqs. (4a)–(5)

$$\frac{e\psi}{k_BT} \approx -\sinh^{-1}\left(\frac{\varphi}{2}\frac{N}{Vn_s}\right) - \frac{1}{2}\frac{\varphi}{\varphi_c}\left(\frac{x^2}{l^2} - \frac{1}{3}\right) \tag{11a}$$

$$n_\pm \approx \sqrt{\left(\frac{\varphi}{2}\frac{N}{V}\right)^2 + n_s^2} \pm \frac{\varphi}{2}\frac{N}{V} \tag{11b}$$

where we define $\varphi_c = a/(\pi l_B)$ as a critical charge fraction, and $l_B = e^2/(4\pi\epsilon_0\epsilon_r k_B T)$ is the Bjerrum length.[31] The derivation of Eq. (11a) follows the procedure presented in the Appendix of Ref. [32]. Combining Eq. (11) and Eq. (3) yields the electrostatic free energy

$$\frac{F_{elec}}{k_BT} \approx \varphi N \sinh^{-1}\left(\frac{\varphi N}{2Vn_s}\right) + 2Vn_s - \sqrt{(\varphi N)^2 + (2Vn_s)^2} \tag{12}$$

As the salt concentration increases, the EDL thickness decreases because the higher ionic strength enhances the electrostatic screening. Consequently, the Debye length can become smaller than the distance between monomers, $\lambda \ll l$, leading to non-overlapping EDLs. At high salt concentrations, the strong screening typically leads to a weak electrostatic potential, $|e\psi| \ll k_BT$, so Eq. (4) can be linearized within the DH limit and gives

$$\frac{d^2\psi}{dx^2} = \frac{2e^2 n_s \psi}{\epsilon_0 \epsilon_r k_B T} \tag{13}$$

Solving Eqs. (13) and (4b) under the boundary condition Eq. (5), we derive approximations for ψ and $n_\pm$

$$\frac{e\psi}{k_BT} \approx -\sqrt{\frac{\varphi^2}{\varphi_c}\frac{N}{2Vn_s}} \frac{\cosh\left(\sqrt{\frac{2Vn_s}{\varphi_c N}}\frac{x}{l}\right)}{\sinh\sqrt{\frac{2Vn_s}{\varphi_c N}}} \tag{14a}$$

$$n_\pm \approx n_s\left(1 \mp \frac{e\psi}{k_BT}\right) \tag{14b}$$

Substituting Eq. (14) into Eq. (3) yields

$$\frac{F_{elec}}{k_BT} \approx \frac{\varphi N}{2}\sqrt{\frac{\varphi^2}{\varphi_c}\frac{N}{2Vn_s}} \tag{15}$$

In the following, we derive three distinct scaling regimes via asymptotic analysis of the Debye length λ and the electrostatic potential ψ.

Regime I. For scenarios of overlapping EDLs $\lambda \gg l$ and beyond DH limit $|e\psi| \gg k_BT$, the large electrostatic potential corresponds to $\varphi N/(2Vn_s) \gg 1$. In this limit $\varphi N/(2Vn_s) \gg 1$, the leading order of Eq. (11a) is $e\psi/(k_BT) \approx -\sinh^{-1}[\varphi N/(2Vn_s)]$, which yields $|e\psi| \gg k_BT$. Therefore, Eq. (12) reduces to

$$\frac{F_{elec}}{k_BT} \approx \varphi N \sinh^{-1}\left(\frac{\varphi N}{2Vn_s}\right) \tag{16}$$

Substituting Eqs. (1) and (16) into $F \approx F_{els} + F_{elec}$ and minimizing the total free energy F with respect to V, we derive the swelling ratio at equilibrium state

$$\frac{V}{Nv} \approx (\varphi N_{str})^{\frac{3}{2}}, \text{for } n_s \ll n_{s1} \tag{17}$$

where $n_{s1} = 1/(4\varphi^{1/2} N_{str}^{3/2} v)$ defines the crossover salt concentration, and $n_s \ll n_{s1}$ corresponds to $|e\psi| \gg k_BT$. Combining Eqs. (17) and (10), we obtain

$$\frac{Gv}{k_BT} \approx \left(\frac{1}{\varphi N_{str}^3}\right)^{\frac{1}{2}}, \text{for } n_s \ll n_{s1} \tag{18}$$

In this asymptotic regime, the contribution of added salt becomes negligible and the swelling is dominated by counterions, consistent with the classical salt-free limit.

Regime II. For scenarios of overlapping EDLs $\lambda \gg l$ and within DH limit $|e\psi| \ll k_BT$, Eq. (12) can be simplified as

$$\frac{F_{elec}}{k_BT} \approx \frac{\varphi^2 N^2}{4Vn_s} \tag{19}$$

Similarly, we minimize F with respect to V and obtain another scaling law

$$\frac{V}{Nv} \approx \left(\frac{\varphi^2 N_{str}}{4vn_s}\right)^{\frac{3}{5}}, \text{for } n_{s1} \ll n_s \ll n_{s2} \tag{20}$$

where $n_{s2} = 2^{11/2}\varphi_c^{5/2}/\left(\varphi^3 N_{str}^{3/2} v\right)$, and $n_s \ll n_{s2}$ is equivalent to $\lambda \gg l$. Substituting Eq. (20) into Eq. (10) yields

$$\frac{Gv}{k_BT} \approx \left(\frac{4vn_s}{\varphi^2 N_{str}^6}\right)^{\frac{1}{5}}, \text{for } n_{s1} \ll n_s \ll n_{s2} \tag{21}$$

Regime III. For scenarios of non-overlapping EDLs $\lambda \ll l$ and within DH limit $|e\psi| \ll k_BT$, substituting Eqs. (1) and (15) into $F \approx F_{els} + F_{elec}$ and minimizing F with respect to V, we obtain the equilibrium swelling ratio of PE gels:

$$\frac{V}{Nv} \approx \left(\frac{\varphi}{2}\right)^{\frac{12}{7}} \left(\frac{N_{str}^2}{2\varphi_c v n_s}\right)^{\frac{3}{7}}, \text{for } n_{s2} \ll n_s \ll n_{s3} \tag{22}$$

where $n_{s3} = 3^{7/8}\varphi^4 N_{str}^{9/8}/(32\varphi_c v)$. For $n_s \ll n_{s3}$ and $n_s \gg n_{s3}$, the free energy is governed by $F_{els} + F_{elec}$ and $F_{els} + F_{EV}$, respectively. Together with Eqs. (22) and (10), we obtain the corresponding modulus in this regime

$$\frac{Gv}{k_BT} \approx \left(\frac{2}{\varphi}\right)^{\frac{4}{7}} \left(\frac{2\varphi_c v n_s}{N_{str}^9}\right)^{\frac{1}{7}}, \text{for } n_{s2} \ll n_s \ll n_{s3} \tag{23}$$

As the Debye length λ decreases with increasing salt concentration n_s, ionic excluded-volume interactions become significant when the ionic volume fraction approaches unity. In this study, these interactions are neglected since ions are treated as point-like particles. However, in the presence of excess salt, the polymer excluded-volume effects become dominant over the electrostatic interactions, causing the charged polyelectrolyte gel to exhibit neutral-like behavior.

Neutral Polymer Gels: $F \approx F_{els}+F_{EV}$

With further increasing salt concentration, the charged monomers experience enhanced ionic screening, resulting in a substantial reduction of the electrostatic free energy F_{elec}. Therefore, when n_s exceeds n_{s3}, the electrostatic interactions become negligible compared with the polymer excluded-volume effect, *i.e.*, $F_{elec} \ll F_{EV}$. As a result, the swelling behavior of the PE gel approaches that of a neutral polymer gel.

Combining Eqs. (1) and (2), and minimizing the total free energy F, we obtain the swelling ratio

$$\frac{V}{Nv} \approx \begin{cases} \left(\frac{N_{str}}{3}\right)^{\frac{3}{8}}, \text{for } \theta \text{ solvent} \\ \left[\left(\frac{1}{2} - \chi\right) N_{str}\right]^{\frac{3}{5}}, \text{for non-}\theta \text{ solvent} \end{cases} \tag{24}$$

In the following discussion, we focus on the θ-solvent case. Substituting the corresponding expression in Eq. (24) into Eq. (10) gives

$$\frac{Gv}{k_BT} \approx \left(\frac{3}{N_{str}^9}\right)^{\frac{1}{8}}, \text{for } n_s \gg n_{s3} \tag{25}$$

Fig. 2 shows the predictions of swelling ratio $V/(Nv) = 1/\phi$ and modulus $Gv/(k_BT)$ at equilibrium state for a PE gel. As the salt concentration increases, the swelling ratio and modulus traverse Regime I–III, and eventually enter the neutral-gel regime. In addition to the widely reported scaling laws in the overlapping EDLs regime (Regime I–II), we predict a new scaling regime $V/(Nv) \propto \varphi^{12/7} n_s^{-3/7}$, $Gv/(k_BT) \propto \varphi^{-4/7} n_s^{1/7}$, which emerges when the EDLs are non-overlapping.

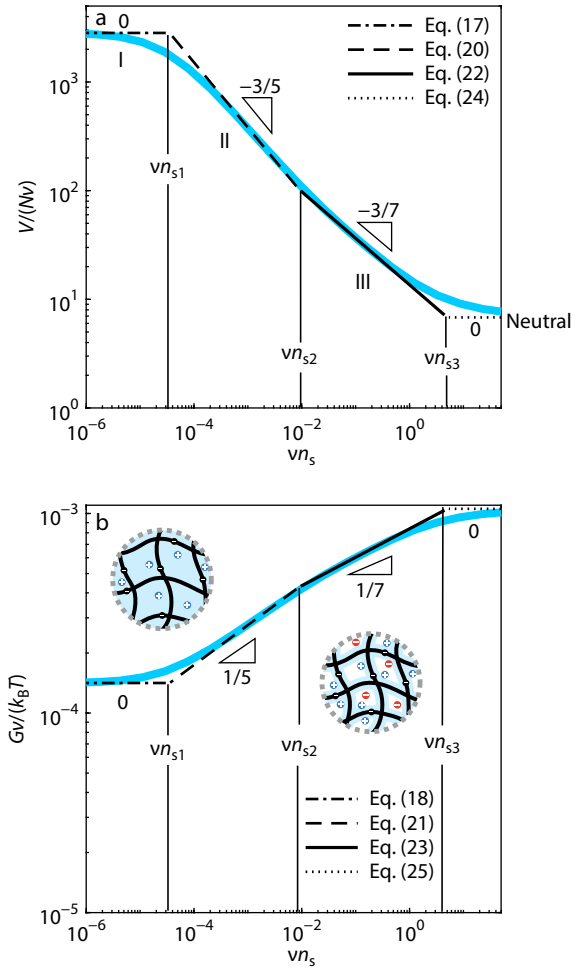

Fig. 2 Theoretical predictions of (a) equilibrium swelling ratio $V/(Nv)$ and (b) dimensionless shear modulus $Gv/(k_BT)$ as a function of dimensionless salt concentration vn_s. The blue solid lines represent the numerical solution for $V/(Nv)$ and $Gv/(k_BT)$ at $\varphi_c = 0.45$. The parameters are $\varphi = 0.4$, $N_{str} = 500$, $v = 10^{-28}$ m^3 and $\chi = 0.5$.

DISCUSSION

Effect of Cross-link Density

The cross-link density of the PE gel is characterized by the monomer number between adjacent cross-links N_{str}, *i.e.*, the strand length. For the gel with larger strand length between the cross-links, the cross-link density is smaller, resulting in a softer network. In contrast, the gel with shorter network strands contains more cross-links per chain and is therefore stiffer.

We compare the swelling behavior of PE gels with different cross-link densities, as shown in Fig. 3(a). Notably, for the stiffer PE gel ($N_{str} = 100$), the swelling curve does not exhibit the scaling behavior $V/(Nv) \propto n_s^{-3/7}$ predicted for Regime III. In this case, the higher cross-link density suppresses the deformation of the gel, so the stiffer gel exhibits a smaller swelling ratio $V/(Nv)$ and a higher monomer density N/V. Consequently, the smaller inter-monomer spacing leads to overlapping EDLs, preventing the system from entering Regime III with non-overlapping EDLs.

In contrast, for softer PE gel ($N_{str} = 500$), the lower cross-link density imposes weaker constraints on network deformation, allowing the gel to undergo much larger deformation under comparable electrostatic interactions. Therefore, with increasing ionic screening, the EDLs of the softer PE gel convert from overlapping to non-overlapping, giving rise to four distinct

https://doi.org/10.1007/s10118-026-3662-1

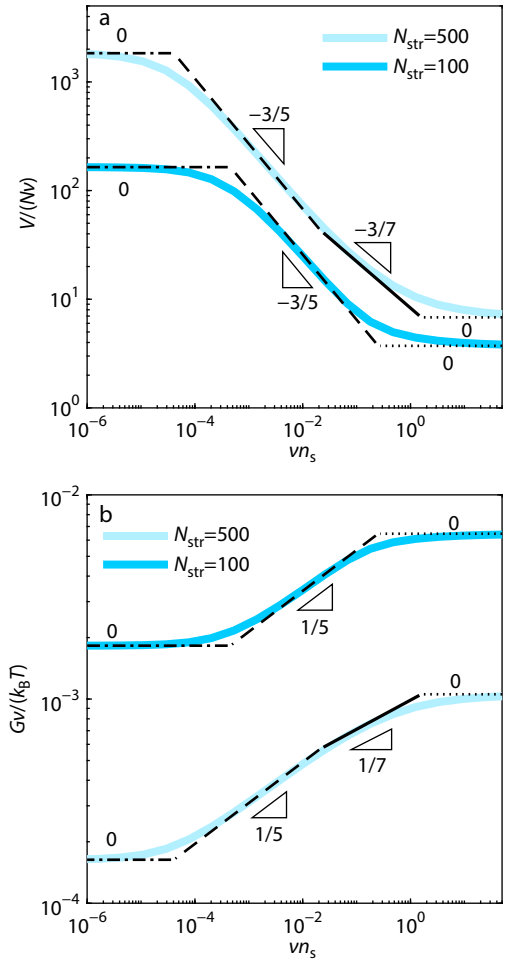

Fig. 3 Theoretical predictions of (a) swelling ratio $V/(Nv)$ and (b) dimensionless shear modulus $Gv/(k_BT)$ at equilibrium state of PE gels with different cross-link densities. The blue solid lines represent the numerical solutions considering $\varphi_c = 0.45$. The dash-dot line, dashed line, solid line and dotted line represent the four distinct scaling laws, respectively. The common parameters are $\varphi = 0.3$, $v = 10^{-28}$ m^3 and $\chi = 0.5$.

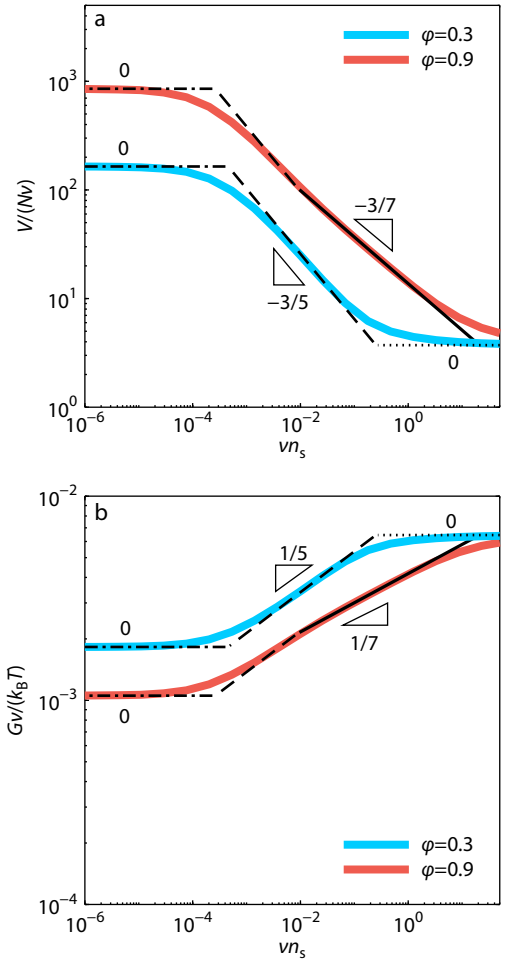

Fig. 4 Theoretical predictions of (a) swelling ratio $V/(Nv)$ and (b) dimensionless shear modulus $Gv/(k_BT)$ at equilibrium state of PE gels with different charge fractions. The red and blue solid lines represent the numerical solutions considering $\varphi_c = 0.45$. The dash-dot line, dashed line, solid line and dotted line represent the four distinct scaling laws, respectively. The common parameters are $N_{str} = 100$, $v = 10^{-28}$ m^3 and $\chi = 0.5$.

scaling regimes.

Theoretical predictions of the dimensionless shear modulus $Gv/(k_BT)$ for two kinds of gels are shown in Fig. 3(b). The PE gel with smaller N_{str}, corresponding to a higher cross-link density, exhibits a significantly larger shear modulus. This behavior is fully consistent with the general notion that polymer networks with higher cross-link density are stiffer.

Effect of Charge Fraction

We then compare the swelling behavior and modulus of PE gels with different charge fraction φ, as shown in Fig. 4. We find that the weakly charged gel with $\varphi = 0.3 < \varphi_c$ doesn't exhibit the scaling law of Regime III, whereas for the strongly charged gel with $\varphi = 0.9 > \varphi_c$, Regime III fits well over a broad range of salt concentrations. In addition, the scaling law $V/(Nv) \propto n_s^{-3/5}$ of Regime II dominates the swelling behavior of weakly charged gels at intermediate salt concentrations, while for strongly charged gels, Regime II is not well captured by the numerical solution.

These differences arise from the different electrostatic interaction strengths within two kinds of PE gels. In strongly charged gels, each monomer carries a larger average charge, resulting in stronger electrostatic repulsion between adjacent monomers. Thus, at a given salt concentration, strongly charged gels exhibit a larger equilibrium swelling ratio. Meanwhile, owing to the stronger electrostatic interactions within strongly charged gels, the electrostatic free energy remains significant, and the neutral-gel regime is therefore not observed.

The new scaling relation $V/(Nv) \propto \varphi^{12/7} n_s^{-3/7}$ in Regime III provides a clear criterion to identify whether the EDLs within the PE gel remain overlapping or become non-overlapping. According to the above discussions, this regime is more readily accessed in weakly cross-linked PE gels, such as mucus. The transition from overlapping to non-overlapping EDLs alters the effective range of electrostatic interactions within the gel, which affects the mechanical and rheological response of PE gels. Furthermore, the distinct scaling enables estimation of gel parameters, such as cross-link density and effective

https://doi.org/10.1007/s10118-026-3662-1

charge fraction, from experimental data.

CONCLUSIONS

We presented a unified theoretical framework to elucidate the salt-dependent swelling behavior and shear modulus of polyelectrolyte gels. Our cell model captures the essential role of electrostatic screening and inter-monomer interactions, and reveals how distinct scaling regimes emerge across overlapping and non-overlapping electric double layers. In addition to the two scaling laws previously reported in the overlapping EDLs regime, we report a new scaling law $V/(Nv) \propto \varphi^{12/7} n_s^{-3/7}$ in the non-overlapping EDLs regime. This scaling regime arises only at sufficiently low cross-link density, high charge fraction and high salt concentration, and therefore can be particularly significant for soft PE gels, such as biological mucus. Furthermore, we compare the swelling behavior and modulus of PE gels with different cross-link densities and charge fractions. We anticipate our model will facilitate the interpretation of experimental observations and provide guidance for the design and applications of stimuli-responsive polyelectrolyte gels.

Conflict of Interests

The authors declare no interest conflict.

Data Availability Statement

The data supporting the findings of this study are available within the article. Additional data are available from the corresponding author upon reasonable request.

ACKNOWLEDGMENTS

This work was financially supported by the National Natural Science Foundation of China (No. U25B20129), the Beijing Natural Science Foundation (No. QY25111) and the Self-made Experimental Instruments and Equipment Project of Shenzhen Technology University (No. JSZZ202301004).

REFERENCES

1 Horkay, F. Polyelectrolyte gels: a unique class of soft materials. *Gels* **2021**, *7*, 102.
2 Harland, R. S.; Prud'homme, R. K., in *Polyelectrolyte gels: properties, preparation, and applications*. American Chemical Society, Washington, DC, **1992**, p. 2.
3 Wilcox, K. G.; Kozawa, S. K.; Morozova, S. Fundamentals and mechanics of polyelectrolyte gels: thermodynamics, swelling, scattering, and elasticity. *Chem. Phys. Rev.* **2021**, *2*, 041309.
4 Quesada-Pérez, M.; Maroto-Centeno, J. A.; Forcada, J.; Hidalgo-Alvarez, R. Gel swelling theories: the classical formalism and recent approaches. *Soft Matter* **2011**, *7*, 10536.
5 Xin, C.; Jin, D.; Hu, Y.; Yang, L.; Li, R.; Wang, L.; Ren, Z.; Wang, D.; Ji, S.; Hu, K.; Pan, D.; Wu, H.; Zhu, W.; Shen, Z.; Wang, Y.; Li, J.; Zhang, L.; Wu, D.; Chu, J. Environmentally adaptive shape-morphing microrobots for localized cancer cell treatment. *ACS Nano* **2021**, *15*, 18048–18059.
6 Zheng, Z.; Wang, H.; Dong, L.; Shi, Q.; Li, J.; Sun, T.; Huang, Q.; Fukuda, T. Ionic shape-morphing microrobotic end-effectors for environmentally adaptive targeting, releasing, and sampling. *Nat. Commun.* **2021**, *12*, 411.
7 Park, N.; Kim, J. Hydrogel-based artificial muscles: overview and recent progress. *Adv. Intell. Syst.* **2020**, *2*, 1900135.
8 Shao, Z.; Wu, S.; Zhang, Q.; Xie, H.; Xiang, T.; Zhou, S. Salt-responsive polyampholyte-based hydrogel actuators with gradient porous structures. *Polym. Chem.* **2021**, *12*, 670–679.
9 Gladman, A. S.; Matsumoto, E. A.; Nuzzo, R. G.; Mahadevan, L.; Lewis, J. A. Biomimetic 4D printing. *Nat. Mater.* **2016**, *15*, 413–418.
10 Dong, Y.; Wang, S.; Ke, Y.; Ding, L.; Zeng, X.; Magdassi, S. 4D printed hydrogels: fabrication, materials, and applications. *Adv. Mater. Technol.* **2020**, *5*, 2000034.
11 Flory, P. J.; Rehner, J. Statistical mechanics of cross-linked polymer networks I. Rubberlike elasticity. *J. Chem. Phys.* **1943**, *11*, 512–520.

Graphical Abstract

Influence of Salt on Swelling and Modulus of Polyelectrolyte Gels

Yi-Ming Liu, Jia-Dong Chen, Xian-Zhao Huang, Zhi-Xing Zhang, and Guang Chen

Peking University; Shenzhen Technology University

Polyelectrolyte gels exhibit salt-responsive swelling behavior due to electrostatic interactions between charged monomers and mobile ions. Using a cell model that explicitly addresses inter-monomer electrostatic interactions, we investigate the salt-dependent swelling and shear modulus of polyelectrolyte gels, and reveal four distinct scaling regimes covering both overlapping and non-overlapping electric double layers.

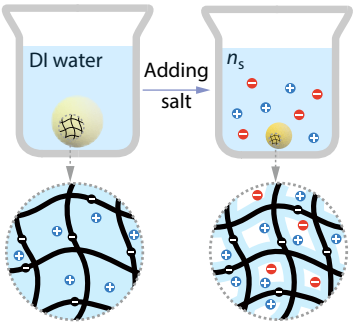

Chinese J. Polym. Sci., 2026 *https://doi.org/10.1007/s10118-026-3662-1*

12 Flory, P. J.; Rehner, J. Statistical mechanics of cross-linked polymer networks II. Swelling. *J. Chem. Phys.* **1943**, *11*, 521–526.
13 Fuoss, R. M.; Katchalsky, A.; Lifson, S. The potential of an infinite rod-like molecule and the distribution of the counter ions. *Proc. Natl. Acad. Sci. U.S.A.* **1951**, *37*, 579–589.
14 Katchalsky, A.; Michaeli, I. Polyelectrolyte gels in salt solutions. *J. Polym. Sci.* **1955**, *15*, 69–86.
15 Yin, Y. Swelling behavior of polyelectrolyte gels. Thesis, Princeton University, **1993**.
16 Landsgesell, J.; Sean, D.; Kreissl, P.; Szuttor, K.; Holm, C. Modeling gel swelling equilibrium in the mean field: from explicit to Poisson–Boltzmann models. *Phys. Rev. Lett.* **2019**, *122*, 208002.
17 Flory, P. J., in *Principles of Polymer Chemistry*, Cornell University Press, Ithaca, **1953**, pp. 584–593.
18 Ricka, J.; Tanaka, T. Swelling of ionic gels: quantitative performance of the Donnan theory. *Macromolecules* **1984**, *17*, 2916–2921.
19 Rubinstein, M.; Colby, R. H. Elastic modulus and equilibrium swelling of polyelectrolyte gels. *Macromolecules* **1996**, *29*, 398–406.
20 Hong, W.; Zhao, X.; Suo, Z. Large deformation and electrochemistry of polyelectrolyte gels. *J. Mech. Phys. Solids* **2010**, *58*, 558–577.
21 Hua, J.; Mitra, M. K.; Muthukumar, M. Theory of volume transition in polyelectrolyte gels with charge regularization. *J. Chem. Phys.* **2012**, *136*, 134901.
22 Jia, D.; Muthukumar, M. Theory of charged gels: swelling, elasticity, and dynamics. *Gels* **2021**, *7*, 49.
23 Duan, M.; Chen, J.; Liu, Y.; Peng, Z.; Chen, G. Swelling of spherical polyelectrolyte gels. *Chinese J. Polym. Sci.* **2024**, *42*, 1386–1392.
24 Lodge, T. P.; Hiemenz, P. C., in *Polymer chemistry*, 3rd ed., CRC Press, Boca Raton, **2020**, pp. 439–475.
25 Doi, M., in *Soft matter physics*, Oxford University Press, Oxford New York, **2013**, pp. 16–48.
26 Zheng, B.; Avni, Y.; Andelman, D.; Podgornik, R. Charge regulation of polyelectrolyte gels: swelling transition. *Macromolecules* **2023**, *56*, 5217–5224.
27 Dobrynin, A.; Rubinstein, M. Theory of polyelectrolytes in solutions and at surfaces. *Prog. Polym. Sci.* **2005**, *30*, 1049–1118.
28 Cano, T.; Na, H.; Sun, J. Y.; Kim, H. Y. Swelling kinetics of constrained hydrogel spheres. *Soft Matter* **2023**, *19*, 8820–8831.
29 Butler, M. D.; Montenegro-Johnson, T. D. The swelling and shrinking of spherical thermo-responsive hydrogels. *J. Fluid Mech.* **2022**, *947*, A11.
30 de Gennes, P. G., in *Scaling concepts in polymer physics*, Cornell University Press, Ithaca, **1979**, pp. 69–76.
31 Chen, G.; Perazzo, A.; Stone, H. A. Influence of salt on the viscosity of polyelectrolyte solutions. *Phys. Rev. Lett.* **2020**, *124*, 177801.
32 Chen, G.; Perazzo, A.; Stone, H. A. Electrostatics, conformation, and rheology of unentangled semidilute polyelectrolyte solutions. *J. Rheol.* **2021**, *65*, 507–526.
33 Chen, J.; Duan, M.; Zhang, R.; Chen, G. A scaling theory for polyelectrolyte brushes: insights from inter-monomer electrostatic interactions. *Macromolecules*, **2026**, doi: 10.1021/acs.macromol.6c00048.
34 Zhang, R.; Duan, M.; Chen, J.; Chen, G. Ionization of semidilute weak polyelectrolytes in equilibrium with a reservoir. *Macromolecules*, **2026**, doi: 10.1021/acs.macromol.5c03101.
35 Chester, S. A.; Anand, L. A coupled theory of fluid permeation and large deformations for elastomeric materials. *J. Mech. Phys. Solids* **2010**, *58*, 1879–1906.